Adsorption 3, 117–125 (1997)

Charge Dynamics of a Methane Adsorption Storage System: Intraparticle Diffusional Effects

J.P. BARBOSA MOTA
Instituto de Biologia Experimental e Tecnológica, Apartado 12, P-2780 Oeiras, Portugal

A.E. RODRIGUES
Laboratory of Separation and Reaction Engineering, School of Engineering, University of Porto, P-4099 Porto Codex, Portugal

E. SAATDJIAN
Laboratoire d'Energétique et de Mécanique Théorique et Appliquée, ENSEM, 2 avenue de la Forêt de Haye, B.P. 160, F-54504 Vandoeuvre Cedex, France

D. TONDEUR
Laboratoire des Sciences du Génie Chimique–CNRS, ENSIC, 1 rue Grandville, B.P. 451, F-54001 Nancy Cedex, France

Received February 8, 1996; Revised June 13, 1996; Accepted July 10, 1996

Abstract. The charge of natural gas adsorption storage systems is studied numerically, with emphasis given to the impact on its dynamics of intraparticle diffusional resistances to mass transport. Besides adsorption kinetics and thermal effects, the simulation model takes into account both mass transport inside the adsorbent and hydrodynamics of flow through the packed bed. Numerical results are presented for charge with methane of a 50 liter cylindrical reservoir, filled with hypothetical adsorbents with diffusional time constants in the range $10^{-3}\ s^{-1} \leq D/R_p^2 \leq \infty$, and with the adsorption equilibrium curve of a commercially available activated carbon with a good adsorptive storage capacity. An attempt is made to assemble the charge histories for different values of D/R_p^2 in a single curve by using a modified time scale.

Keywords: methane adsorption, on-board storage, mathematical modeling, numerical simulation

1. Introduction

Natural gas (NG) is a potentially attractive fuel for vehicle use. It is cheaper than gasoline or diesel and NG vehicles have a less adverse effect on environment than vehicles running on those fuels, emitting less carbon dioxide, a major greenhouse gas, as well as several other air polluants (Talu, 1992). The technical feasibility of NG vehicles is well established. Several countries already have natural gas fleets and ongoing research and development programs (Penilla et al., 1994). One point mentioned in the task force "The car of Tomorrow" of the European Commission's Green Paper on Innovation (1995) is that "... in the medium term, vehicles running on compressed natural gas will have a major role."

Natural gas is about 95% methane, a gas that cannot be liquefied at ambient temperature ($T_c = 190.6$ K). Therefore, its compact storage on a vehicle has required the use of high-pressure compression technology

(16.5–20.7 MPa), which is expensive and heavy (Jasionowski et al., 1989). All efforts to improve this technology have focused on lowering storage pressure in order to decrease capital and operating costs of compression stations, and allow the use of lighter on-board gas storage reservoirs. A promising low-pressure (<4 MPa) system for storing NG is adsorption storage, it is a good compromise between compression costs and on-board storage capacity (Remick and Tiller, 1985; Talu, 1992).

Most research on adsorbed natural gas (ANG) has focused on the development and evaluation of economical adsorbents with storage capacities comparable to that of compressed NG (Barton et al., 1983, 1987; Chahine and Bose, 1992; Czepirski, 1991; Quinn, 1990; Quinn and MacDonald, 1992; Quinn et al., 1994; Remick et al., 1984; Sejnoha, 1994). A common ANG storage performance indicator is volumes of stored NG, measured at standard conditions, per storage volume (v/v). The highest experimental storage capacities obtained to date (at 3.5 MPa and 25°C) are for the high performance, but expensive, activated carbon AX-21: 101 v/v for granulated particles and 144 v/v for a mixture of carbon with polymeric binder, pressed into the desired geometrical shape under mechanical pressure and then dried (Sejnoha et al., 1994). However, good capacities (82 v/v and 103 v/v) were also obtained by the same authors with a much cheaper, commercially available carbon (CNS). Grand canonical Monte Carlo molecular simulations predict that the theoretical maximum storage capacity is 209 v/v for monolithic carbon and 146 v/v for pelletized carbon (Matranga et al., 1992). These values may be compared to 240 v/v for compressed NG at 20.7 MPa.

Several problems that affect the success of ANG technology have been addressed in the literature. One of them is the loss due to the residual amount of NG left at depletion, which can be as high as 30% of the amount stored at charge conditions (BeVier et al., 1989; Matranga et al., 1992; Talu, 1992, 1993). This is a consequence of the shape of the adsorption isotherm and the unfeasibility of lowering storage pressure below atmospheric.

Another problem is the management of thermal effects, related to the heat of adsorption, which adversely affect ANG storage (BeVier et al., 1989; Jasionowski et al., 1989; Remick and Tiller, 1986; Sejnoha et al., 1994). If the heat of adsorption released during charge is not removed from the storage system, less methane is adsorbed as the substrate heats up. When the heat of adsorption is not resupplied during discharge, the temperature drops, increasing the residual amount of NG that remains in storage at depletion. The penalty in both phases can be very high.

Yet another problem that has received attention in the literature is the gradual contamination of the adsorbent with heavy hydrocarbons and water vapor present in natural gas (BeVier et al., 1989; Sejnoha et al., 1994; Talu, 1992, 1993). If these are allowed to enter the on-board storage system, they can adsorb preferentially to high equilibrium residual levels and decrease storage capacity. However, the presence of impurities is not always prejudicial; the introduction into the reservoir of a judiciously chosen additive might even increase net storage capacity (Talu, 1993). This is true if the impact of the additive on the amount of NG adsorbed at depletion pressure is higher than at charge pressure.

Recently, Mota (1995), Mota et al. (1993, 1995) developed a two-dimensional model describing the dynamics of ANG storage in cylindrical reservoirs. Both charge and discharge phases were studied. A simple formula was proposed to predict the filling time when the packed bed is the only resistance to gas flow. The predicted temperature changes in the reservoir are in good agreement with those reported in the literature for an experimental charge/discharge. In this work, an intraparticle transport equation governed by a diffusional law is added to our previous model, where intraparticle and film resistances to both heat and mass transfer were neglected, in order to extend its applicability and study the influence of diffusional resistances on the dynamics of the storage system.

High storage densities can only be achieved if practically all stored methane is in the adsorbed phase. The void space where methane is at gas density can be minimized by producing the carbon as a monolith or as shaped pieces that nest together. Since methane adsorption at ambient temperature is principally a micropore phenomenon, most of the intraparticle void volume should be micropore. This, in turn, may increase significantly the intraparticle diffusional resistances to mass transport and, consequently, lead to unacceptable filling times. The diffusional model might also be useful for studying the performance of storage systems employing zeolites, since these adsorbents have diffusional time constants, $D/R_p^2 \approx 10^{-3}\ s^{-1}$, which are smaller than those for activated carbons, $D/R_p^2 \approx 10^{-1}\ s^{-1}$ (Yang, 1987). In spite the fact that carbons are better adsorbents for natural gas on weight basis, the difference between carbon and zeolite

performance is much smaller on volumetric basis since zeolites have higher density than carbons (Talu, 1992).

2. Problem Formulation and Solution

The system under study is depicted in Fig. 1. It consists of a cylindrical reservoir filled with a homogeneous packed bed of adsorbent particles. The gas enters and leaves the tank through a small opening located in the center of the cylinder's front face. The assumptions, on which the equilibrium model developed previously (Mota et al., 1995) is based, are retained here, except for the presence of a non-negligible intraparticle diffusional resistance to mass transport.

It is assumed that the adsorbent particles can be approximated by equivalent spheres of radius R_p. This makes the intraparticle profiles dependent only on the radial coordinate, r_p, of the particles. In this case, the differential mass balance on a spherical shell element of a particle gives

$$\frac{\partial}{\partial t}(c_p^* + q^*) = \frac{D/R_p^2}{x^2}\frac{\partial}{\partial x}\left(x^2\frac{\partial q^*}{\partial x}\right), \qquad 0 < x \equiv r_p/R_p < 1, \quad (1)$$

where $c_p^* \equiv \epsilon_p c_p$ and $q^* = \rho_b q/(1-\epsilon)$.

In principle, the effective diffusion coefficient, D, for transport of a single species in the absence of intraparticle temperature gradients is

$$D = D_s + \left(D_{Ke} + \frac{B_o P_p}{\mu}\right)\frac{\partial c_p^*}{\partial q^*}, \quad (2)$$

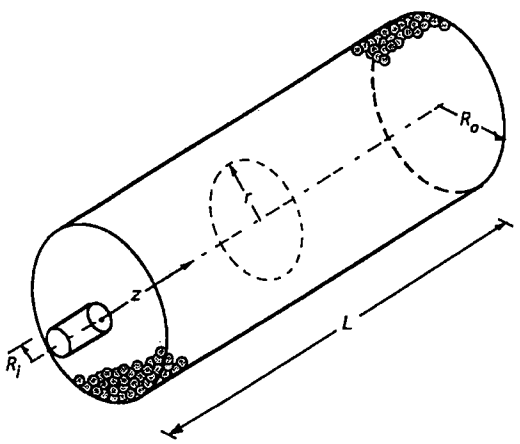

Figure 1. Schematic diagram of reservoir and coordinate system.

where B_o is the permeability of the particle, D_{Ke} is the effective Knudsen diffusivity, and D_s accounts for surface or micropore diffusion depending on pore size. The Knudsen and viscous contributions to total flux can be reasonably estimated, although there remains some uncertainty in predicting the tortuosity factor. Surface and micropore diffusivities are more difficult to predict theoretically and any reasonable model should be based on experimental data. Since the present work is focused on highly microporous activated carbons or zeolites, where surface concentration is high ($\partial c_p^*/\partial q^* \ll 1$), it seems likely that most of the intraparticle mass transport being modeled occurs through the adsorbed phase (D_s), where most of the predictive uncertainty lies. The approach adopted here is the simplest one: symbol D denotes the effective diffusivity whose value is considered constant. As implied by (1), D is based on the adsorbed phase concentration gradient.

The values of c_p and q are related to intraparticle pressure and temperature by the ideal gas law,

$$c_p = P_p M_g/(RT_p), \quad (3)$$

and by the adsorption equilibrium relation,

$$q = q_{eq}(P_p, T_p). \quad (4)$$

In the present work, the equilibrium relation is of Langmuir type and is based on experimental data published by Remick and Tiller (1986) for an activated carbon with a good NG adsorptive storage capacity:

$$\begin{aligned} q_{eq} &= (q_m b P)/(1 + bP), \\ q_m &= 55920 T^{-2.3}, \\ b &= 1.0863 \times 10^{-7} e^{806/T}. \end{aligned} \quad (5)$$

Heat transfer is assumed to be sufficiently rapid, relative to sorption rate, so that intraparticle temperature gradients are negligible, i.e., $\partial T_p/\partial x \approx 0$ inside the particles. Previous simulations using a separate intraparticle energy balance with heat transfer resistances concentrated in the external film showed that, for the system studied, the heat transfer resistance introduced by the external film can be neglected. Thus, $T_p = T$ for every particle, where T is the temperature of the gas surrounding it.

For reasons that will become clear when the solution method is discussed, q^* is taken as the dependent variable inside the particles rather than intraparticle

pressure, P_p. Appropriate boundary conditions for q^* are

$$\begin{cases} \partial q^*/\partial x = 0 & \text{for } x = 0 \\ q^* = \rho_b q_{eq}(P, T)/(1-\epsilon) & \text{for } x = 1 \end{cases} \quad (6)$$

The first is simply the mandatory noflux or symmetry condition in the center of the particle, while the second one states that the adsorbed phase at the external surface of the particle is in equilibrium with the surrounding gas. Intraparticle pressure can be eliminated from c_p^* using (3) and (5), giving

$$c_p^* = \frac{\epsilon_p M_g q^*/(RTb)}{q_m^* - q^*}. \quad (7)$$

The equations for the packed bed are formulated in axisymmetric coordinates, (z, r), which are the best suited for the tank geometry since the walls of the cylinders are mapped to constant z or r values.

The continuity equation is written as

$$\frac{\partial}{\partial t}[\epsilon c + (1-\epsilon)(\bar{c}_p^* + \bar{q}^*)] + \nabla \cdot (c\mathbf{v}) = 0, \quad (8)$$

where $\bar{c}_p^*(t, z, r)$ and $\bar{q}^*(t, z, r)$ are averaged values of c_p^* and q^* at time t over a particle located at point (z, r) in the tank. These average values are related to intraparticle profiles by

$$(\bar{c}_p^*, \bar{q}^*) = \frac{1}{V_p}\iiint_{V_p}(c_p^*, q^*)\,dV_p = 3\int_0^1 (c_p^*, q^*)\,x^2\,dx. \quad (9)$$

Concerning the momentum balance, Ergun's equation (Ergun, 1952) is considered locally valid and is extended to two dimensions. The expression written in vector form is

$$\mathbf{v} = -\frac{2\nabla P}{\alpha + \sqrt{\alpha^2 + 4\beta c\|\nabla P\|}}, \quad (10)$$

$$\|\nabla P\| = \left[\left(\frac{\partial P}{\partial z}\right)^2 + \left(\frac{\partial P}{\partial r}\right)^2\right]^{1/2}, \quad (11)$$

$$\alpha = 150(1-\epsilon)^2\mu/(4\epsilon^3 R_p^2), \quad (12)$$

$$\beta = 1.75(1-\epsilon)/(2\epsilon^3 R_p). \quad (13)$$

The energy equation can be written as

$$\frac{\partial}{\partial t}[(\epsilon c + (1-\epsilon)(\bar{c}_p^* + \bar{q}^*))C_{pg}T] + \Delta H\frac{\partial \bar{q}^*}{\partial t} - \epsilon\frac{\partial P}{\partial t} - (1-\epsilon)\epsilon_p\frac{\partial \bar{P}_p}{\partial t} + \rho_b C_{ps}\frac{\partial T}{\partial t} + \nabla \cdot (C_{pg}Tc\mathbf{v} - \lambda_e \nabla T) = 0, \quad (14)$$

with

$$\lambda_e = \lambda_e^o + 2\gamma C_{pg} R_p c\|\mathbf{v}\|, \quad \gamma = 0.3. \quad (15)$$

The energy balance is based on the assumption of constant values of thermodynamic properties and negligible rates of change of kinetic and potential energy of the gas when compared with the rate of change of the system's internal energy. These assumptions are fully justified in Mota et al. (1995).

The boundary conditions at the bed scale are

$$\begin{cases} \mathbf{v} \cdot \mathbf{n} = 0 \\ \lambda_e \nabla T \cdot \mathbf{n} = h_w(T_w - T) \end{cases} \quad \text{for} \begin{cases} z = 0,\ R_i \le r \le R_o \\ 0 \le z \le L,\ r = R_o, \\ z = L,\ 0 \le r \le R_o \end{cases} \quad (16)$$

where $\mathbf{n}$ is the outwards unit vector normal to each point of the walls. By this we are simply stating that there is no gas flow across the lateral wall, front face excluding the opening, and rear face of the cylinder, and that heat transfer to these locations is governed by a wall heat transfer coefficient h_w. In this work, h_w is set to zero (adiabatic operation), which is a good approximation for the charge phase.

Boundary conditions along the longitudinal axis of the reservoir must express the inexistence of radial fluxes, either of mass or heat, i.e.,

$$\frac{\partial P}{\partial r} = 0, \quad \frac{\partial T}{\partial r} = 0 \quad \text{for } 0 \le z \le L,\ r = 0. \quad (17)$$

The following boundary conditions are employed in the opening ($z = 0,\ 0 \le r \le R_i$):

$$P = P_{ext}, \quad \begin{cases} C_{pg}(T_{ext} - T)cv = -\lambda_e(\partial T/\partial z) \\ \text{(during charge)} \\ \partial T/\partial z = 0 \\ \text{(during discharge)} \end{cases} \quad (18)$$

The equations for the packed bed were solved by finite differences using a control volume formulation. In this context the charge boundary condition states that the energy flux at $z = 0^-$ (external pressure source) is oriented axially and its magnitude is $C_{pg}(Tcv)_{ext}$, while at $z = 0^+$ (packed bed side) is $C_{pg}Tc\mathbf{v} - \lambda_e \nabla T$ with $\mathbf{v}$ given by Ergun's equation (10). Notice that $(cv)_{ext}$, i.e., the mass flux of gas entering the reservoir, is calculated by employing (8) at the opening since pressure is fixed there ($P = P_{ext}$). The discharge boundary condition is included for completeness; the work presented here is focused on charge (pressurization), where diffusional resistances may have practical significance. A simulation model addressing the influence of thermal effects on slow discharge is currently under development.

The initial conditions ($t = 0$) inside the reservoir are

$$P(z, r) = P_i, \quad T(z, r) = T_i,$$
$$q^*(z, r, x) = q^*_{eq}(P_i, T_i)$$
$$\text{for } 0 \le z \le L, \ 0 \le r \le R_o, \ 0 \le x \le 1, \quad (19)$$

and refer to a state of uniform pressure and temperature, the latter being equal to the temperature of the external pressure source ($T_i = T_{ext}$).

The problem is solved by first eliminating its dependence on the radial coordinate, r_p, of the particles so that the resulting system contains only ordinary and partial differential equations in the two coordinates (z, r) of the tank. This is accomplished by discretizing (1) using finite differences or some method of weighted residuals. Interior orthogonal collocation (Finlayson, 1972; Villadsen and Stewart, 1967) with a weight function $w(x) = 1$ was employed in this work. In this approach, (1) is replaced by a system of N differential equations,

$$\frac{\partial}{\partial t}(\mathbf{c}^*_p + \mathbf{q}^*) = \left(D/R_p^2\right) B A^{-1} [\mathbf{q}^* - q^*_{eq}(P, T)\mathbf{u}], \quad (20)$$

where N is the number of interior collocation points, $\mathbf{c}^*_p$ and $\mathbf{q}^*$ are vectors holding the values of the respective variables at the collocation points, and $\mathbf{u}$ is a vector with all its elements equal to one. Symbols A and B denote square matrices with entries given by

$$A_{ij} = \left(1 - x_i^2\right) x_i^{2j-2} \quad (j = 1, \ldots, N) \quad (21)$$

and

$$B_{ij} = \begin{cases} -6 & \\ (j = 1) & \\ \left[(2j-2)(2j-1) - (2j)(2j+1)x_i^2\right] x_i^{2j-4} & \\ \qquad (j = 2, \ldots, N) & \end{cases} \quad (22)$$

where $x_1, \ldots, x_N$ are the collocation points.

The average values of c^*_p and q^* are computed from (9) using the quadrature formula

$$\int_0^1 g(x^2)\, x^2 dx = \sum_{j=1}^{N} w_j g\left(x_j^2\right) + w_{N+1} g(1), \quad (23)$$

with a proper selection of the coefficients w_j to increase the accuracy of the formula (Finlayson, 1972).

If $N = 0$ then $\bar{c}_p = c$ and $\bar{q} = q_{eq}(P, T)$, which is just the equilibrium model considered by Mota et al. (1995). If one interior collocation point is employed ($N = 1$), a single intraparticle transport equation is obtained:

$$\frac{\partial}{\partial t}(\bar{c}^*_p + \bar{q}^*) = 15\left(D/R_p^2\right)(q^*_{eq} - \bar{q}^*), \quad (24)$$

which closely resembles the linear driving force approximation (Yang, 1987; Do and Rice, 1986).

The resulting system of $N + 2$ mixed ordinary and partial differential equations, i.e., (8), (13), and (20), is solved using a numerical package developed by the authors for the numerical solution of two-dimensional parabolic partial differential equations associated with transport problems. As mentioned previously, the packaged employs finites differences and is based on a control volume formulation. The reader is referred to Mota (1995) for further details on the numerical package and computational grid employed.

3. Results and Discussion

The reservoir simulated is an ultra-lightweight 50 liter cylinder (87 cm × 28 cm, 13 kg), manufactured by EDO Canada Ltd. for compressed natural gas storage. Table 1 lists the values of fluid, particle and system properties employed in the numerical simulations.

In order to determine the minimum number of collocation points required for the attainment of precise solutions, preliminary runs employing different number of collocations points were made and the results compared. Figure 2 shows plots of total amount of methane

Table 1. Data used in numerical simulations.

C_{pg}	2450 J kg^{-1} K^{-1}	R_p	5×10^{-4} m
C_{ps}	650 J kg^{-1} K^{-1}	T_{ext}	285 K
ΔH	-1.1×10^6 J kg^{-1}	T_i	285 K
L	0.85 m	ϵ	0.3
M_g	16.04×10^{-3} kg mol^{-1}	ϵ_p	0.6
P_{ext}	3.5 MPa	λ_e^o	1.2 J m^{-1} K^{-1} s^{-1}
P_i	0.101 MPa	μ	1.25×10^{-5} kg m^{-1} s^{-1}
R_i	0.005 m	ρ_b	410 kg m^{-3}
R_o	0.14 m		

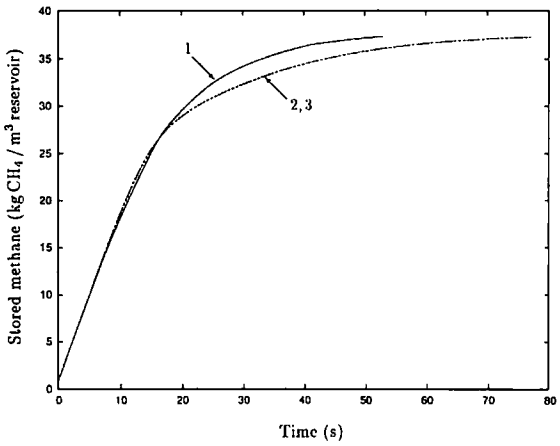

Figure 2. History of total amount of methane stored per unit reservoir volume, during charge, for $D/R_p^2 = 5 \times 10^{-3}$ s^{-1}. Solutions obtained with 1, 2, and 3 collocation points.

stored in the tank versus time, during charge, corresponding to solutions obtained with 1, 2, and 3 collocation points. The weight function used was $w(x^2) = 1$ and the D/R_p^2 value considered was 5×10^{-3} s^{-1}. The curves obtained with 2 and 3 collocation points are superimposed; thus, 2 or 3 collocation points are sufficient in this case. On the other hand, the solution based on a single collocation point underestimates considerably the filling time. Subsequent simulations were all carried out with 3 interior collocation points.

The two-dimensional pressure and temperature fields, during charge, are similar to figures presented in our previous work concerning the equilibrium model (Mota et al., 1995). However, temperature spatial variations are less pronounced in the presence of nonnegligible intraparticle diffusional resistances, because the adsorbent heats up at a slower rate and the system has more time to smooth the temperature front by conduction.

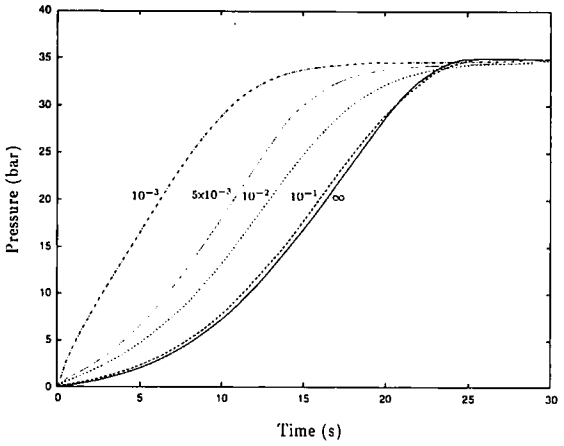

Figure 3. Interparticle pressure history in the center of the reservoir, during charge, for different values of D/R_p^2 (s^{-1}).

Figure 3 shows the interparticle pressure history in the center of the reservoir, during charge, for different values of D/R_p^2. In the presence of important diffusional resistances, the gas penetrates the particles very slowly, and instead accumulates initially in the interparticle void volume. This results in a rapid pressure increase up to practically the nominal filling pressure, governed by hydrodynamics of flow through the packed bed and interparticle void volume. The subsequent filling proceeds with a rate controlled entirely by the diffusion process. During this period, pressure remains at its charge value since all methane that adsorbs is compensated quickly by the external pressure source. As a result, the pressure history is not representative of the filling of the reservoir, and cannot be used to quantify it. In practice, fuel supply at natural gas refueling stations will be controlled by mass flow measurements so that the amount of gas delivered to consumer is known.

The pressure history curve is always bounded by two limiting cases: the lower one is the equilibrium model ($D/R_p^2 \to \infty$), the upper one corresponds to the charge of a bed of nonporous particles with the same diameter ($D/R_p^2 = 0$).

Figures 4 and 5 show, respectively, histories of average temperature and total amount of methane stored per unit reservoir volume, during charge, for different values of D/R_p^2. These average values are calculated using the following formula:

$$\bar{\bar{\phi}} = \frac{2}{R_o^2 L} \int_0^L \int_0^{R_o} \phi(r, z)\, r\, dr\, dz. \qquad (25)$$

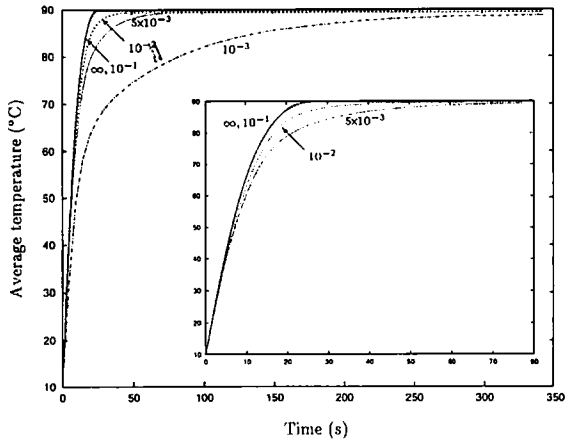

Figure 4. Average temperature history in the reservoir, during charge, for different values of D/R_p^2 (s^{-1}). The inner graphic is an enlargement of the curves (excluding $D/R_p^2 = 10^{-3}\ s^{-1}$) in the short time region.

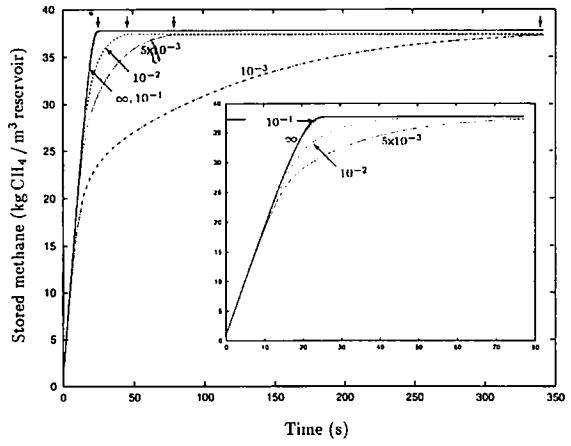

Figure 5. History of total amount of methane stored per unit reservoir volume, during charge, for different values of D/R_p^2 (s^{-1}). The inner graphic is an enlargement of the curves (excluding $D/R_p^2 = 10^{-3}\ s^{-1}$) in the short time region. The vertical arrows in the top of the figure locate the filling times.

The dummy variable ϕ stands for T in the average temperature calculation. When the quantity of interest is the amount of stored methane, ϕ is replaced by $\epsilon c + (1-\epsilon)(\bar{c}_p^* + \bar{q}^*)$. It is clear that for D/R_p^2 values smaller than $10^{-2}\ s^{-1}$, the time needed to completely fill the reservoir is considerably longer than for a system with the same characteristics but without diffusional restrictions. Since h_w was set to zero, all charges simulated occur under adiabatic conditions. In this case, the predicted average temperature rise in bed is 79°C. This value is in agreement with experimental values of 78°C and 82°C observed in two independent adiabatic charge experiments. The former was carried out by Sejnoha et al. (1995) on a 71 liter reservoir filled with CNS activated carbon; the latter was performed by Remick and Tiller (1986) on a 1 liter cylinder filled with the activated carbon that gave rise to the adsorption equilibrium relation used in this work (G216 carbon from North American Carbon Inc. of Columbus, Ohio).

It is interesting to incorporate quantitatively the influence of diffusional resistances into the representation of the results obtained so far, by grouping them as a single curve using a modified time scale. This can be accomplished by subtracting a certain time interval t^* from the filling time and multiplying the result by D/R_p^2, therefore assembling all filling times in a single dimensionless value. The quantity t^* is a correction value that takes into account the fact that while pressure is initially rising in the reservoir, a certain amount of gas is adsorbing inside the particles. This corresponds to eliminating the initial time period during which filling is controlled by hydrodynamics of flow through the packed bed and then focusing on the diffusion process only. The time interval t^* is a function of D/R_p^2, and satisfies the condition

$$\lim_{D/R_p^2 \to 0} t_{\text{fill}} \leq t^* \leq \lim_{D/R_p^2 \to \infty} t_{\text{fill}}. \tag{26}$$

The lower limit is the filling time when the packed bed is made of nonporous particles, while the upper one is the filling time given by the equilibrium model.

Both limits can be predicted by the formula developed by Mota et al. (1995) for estimating the filling time when the packed bed is the only resistance to gas flow:

$$t_{\text{fill}} = \frac{W_f}{\pi R_i^2 \sqrt{c_{\text{ext}}(P_{\text{ext}} - P_i)/(\beta\zeta)}}, \tag{27}$$

where $c_{\text{ext}} = P_{\text{ext}} M_g/(RT_{\text{ext}})$, W_f stands for the adiabatic storage capacity of the reservoir, and ζ is an estimate of the mean penetration distance from the opening of the reservoir where the steepest pressure gradients occur. The reader is referred to our previous work for further details. For the radius of the opening considered in this study ($R_i = 5$ mm), ζ takes the value 4.8 mm if the gas adsorbs in the particles and 7.24 mm otherwise. In the range $10^{-3}\ s^{-1} \leq D/R_p^2 \leq 10^{-2}\ s^{-1}$, an average value $\bar{t}^* = 12$ s is sufficient for attaining a reasonable superposition of the charge curves, as shown in Fig. 6.

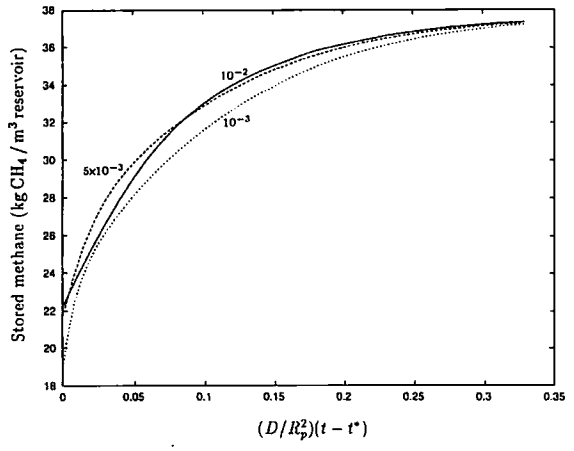

Figure 6. Total amount of methane stored per unit reservoir volume, during charge, as a function of the dimensionless time $(D/R_p^2)(t - t^*)$, for different values of D/R_p^2 (s^{-1}) and $t^* = 12$ s.

4. Conclusions and Final Remarks

The influence of intraparticle diffusional resistances to mass transport on charge dynamics of a methane adsorption storage system was studied numerically. The simulation model takes into account adsorption kinetics, thermal effects, hydrodynamics of flow through the packed bed, and mass transport inside the adsorbent.

When intraparticle diffusional resistances are significant, the pressure history inside the reservoir does not follow the charge curve. The initial pressure rise is governed by hydrodynamics of flow through the packed bed and interparticle void volume. Most of the filling occurs near the nominal charge pressure at a rate controlled by intraparticle diffusional transport. During this period the pressure remains at its charge value since all methane that adsorbs is compensated quickly by the external pressure source.

According to Fig. 5, the filling time when $D/R_p^2 = 10^{-3}$ s^{-1} is nearly 14 times greater than the time required when the storage system has no diffusional limitations. If, in order to reduce void space, the carbon adsorbent is packed as a monolith of high density, an additional resistance to gas flow is introduced and it increases even further the filling time. A measure of this resistance, equivalent to D/R_p^2, is given by $K(P_i + P_{ext})/(2\mu L^2)$, where K is the permeability of the carbon monolith. There must be a limit where further optimizations of micropore structure of the adsorbent and density of the monolith for an increased adsorptive capacity lead to filling times that are too long.

A simulation model for the slow discharge phase is currently under development. This is a problem of practical relevance, because fuel admission to the motor is controlled by the energetic need of the vehicle, and discharge is carried out at much slower rates than when it occurs freely to the atmosphere. It has been shown (Mota, 1995) that the temperature field inside the reservoir remains nearly uniform during a fast discharge. This is a consequence of the practically adiabatic nature of the process and the thermicity being dependent only on the conditions inside the reservoir. When the duration of discharge is increased considerably, the non-uniformity of the temperature field is caused by heat transfer from the surroundings to the packed bed.

Nomenclature

B_o	Permeability of particle (m^2)
c	Interparticle gas concentration (kg m^{-3})
c_p	Intraparticle gas concentration (kg m^{-3})
c_p^*	$\epsilon_p c_p$ (kg m^{-3})
C_{pg}	Heat capacity of gas at constant pressure (J kg^{-1} K^{-1})
C_{ps}	Heat capacity of adsorbent (J kg^{-1} K^{-1})
D	Effective diffusivity (m^2 s^{-1})
h_w	Wall heat transfer coefficient (J m^{-2} K^{-1} s^{-1})
$-\Delta H$	Heat of adsorption (J kg^{-1})
L	Reservoir length (m)
M_g	Molecular mass of gas (kg mol^{-1})
P	Interparticle gas pressure (Pa)
P_{ext}	Charge pressure (Pa)
P_i	Initial pressure in reservoir (Pa)
P_p	Intraparticle gas pressure (Pa)
q	Adsorbed phase concentration (kg kg^{-1})
q^*	$\rho_b q/(1 - \epsilon)$ (kg m^{-3})
q_{eq}	Adsorption equilibrium relation (kg kg^{-1})
r	Radial coordinate in reservoir (m)
r_p	Radial coordinate in particle (m)
R	Ideal gas constant (8.3144 J mol^{-1} K^{-1})
R_i	Radius of opening (m)
R_o	Cylinder radius (m)
R_p	Particle radius (m)
t	Time (s)
t_{fill}	Filling time given by Eq. (27) (s)
T	Interparticle gas temperature (K)
T_{ext}	Temperature of external pressure source (K)
T_i	Initial temperature in reservoir (K)

T_w Wall temperature (K)
$\mathbf{v}$ (v_z, v_r) Superficial velocity vector (m s^{-1})
V_p Particle volume (m^3)
W_f Adiabatic storage capacity of the reservoir (kg)
x Dimensionless radial coordinate in particle
z Axial coordinate in reservoir (m)

Greek Symbols

ϵ Bed porosity
ϵ_p Particle porosity
ζ Length employed in Eq. (27) (m)
λ_e Effective bed thermal conductivity (J m^{-1} K^{-1} s^{-1})
λ_e^o Static bed thermal conductivity (J m^{-1} K^{-1} s^{-1})
μ Viscosity of gas (kg m^{-1} s^{-1})
ρ_b Particle density (kg m^{-3})

Acknowledgments

Financial support received from JNICT (PBIC/P/QUI/2415/95) and from Program PRAXIS XXI (BPD/6066/95) is gratefully acknowledged.

References

Barton, S.S., J.A. Holland, and D.F. Quinn, "Modification of Microporous Carbon for Methane Storage," in *Proceedings of 2nd Int. Conf. on Fundamentals of Adsorption*, A.L. Myers and G. Belfort (Eds.), pp. 99–108, Engineering Foundation Conference, 1987.

Barton, S.S., J.R. Dacey, and D.F. Quinn, "High Pressure Adsorption of Methane on Porous Carbons," in *Proceedings of 1st Int. Conf. on Fundamentals of Adsorption*, A.L. Myers and G. Belfort (Eds.), pp. 65–75, Engineering Foundation Conference, 1983.

BeVier, W.E., J.T. Mullhaupt, F. Notaro, I.C. Lewis, and R.E. Coleman, "Adsorbent-Enhanced Methane Storage for Alternate Fuel Powered Vehicles," presented at *1989 SAE Future Transportation Technology Conference and Exposition*, Vancouver, British Columbia, Aug. 1989.

Chahine, R. and T.K. Bose, "Solidification of Carbon Powder Adsorbents for NGV Storage," presented at *Twentieth Conference on Carbon*, Santa Barbara, CA, June 1992.

Czepirski, L., "Some Aspects of a Sorbent-Containing Storage System for Natural Gas," *Indian J. of Technology*, **29**, 266–268 (1991).

Do, D.D. and R.G. Rice, "Validity of the Parabolic Profile Assumption in Adsorption Studies," *AIChE J.*, **32**, 149–154 (1986).

Ergun, S., "Fluid Flow Through Packed Columns," *Chem. Eng. Prog.*, **42**, 89 (1952).

European Commission, "Green Paper on Innovation," *Bulletin of the European Union*, No. 5/95, Annex 1 (1995).

Finlayson, B.A., *The Method of Weighted Residuals and Variational Principles*, Academic Press, Inc., New York, 1972.

Jasionowski, W.J., A.J. Tiller, J.A. Fata, J.M. Arnold, S.W. Gauthier, and Y.A. Shikari, "Charge/Discharge Characteristics of High-Capacity Methane Adsorption Storage Systems," presented at *1989 International Gas Research Conference*, Tokyo, Japan, Nov. 1989.

Matranga, K.R., A.L. Myers, and E.D. Glandt, "Storage of Natural Gas by Adsorption on Activated Carbon," *Chem. Eng. Sci.*, **47**, 1569–1579 (1992).

Mota, J.P.B., E. Saatdjian, D. Tondeur, and A.E. Rodrigues, "Modeling of a High-Capacity Methane Adsorptive Storage System," in *Proceedings of the Int. Chemical Engineering Conf. CHEMPOR'93*, pp. 159–167, Porto, Portugal, April 1993.

Mota, J.P.B., *Modélisation des Transferts Couplés en Milieux Poreux*, Ph.D. Thesis, Institut National Polytechnique de Lorraine, Nancy, France, 1995.

Mota, J.P.B., E. Saatdjian, D. Tondeur, and A.E. Rodrigues, "A Simulation Model of a High-Capacity Methane Adsorptive Storage System," *Adsorption*, **1**, 17–27 (1995).

Mota, J.P.B., E. Saatdjian, D. Tondeur, and A.E. Rodrigues, "On the Numerical Solution of Partial Differential Equations with Two Spatial Scales," *Comp. & Chem. Eng.*, in press (1996).

Penilla, R.N., J.M.O. Paez, and G.A. Plata, "The Use of Natural Gas," presented at *14th World Petroleum Congress*, Topic 14, Stavanger, Norway, 1994.

Quinn, D.F., "Carbon Adsorbents for Natural Gas," presented at *GURF Meeting*, London, July 1990.

Quinn, D.F. and J.A. MacDonald, "Natural Gas Storage," *Carbon*, **7**, 1097–1103 (1992).

Quinn, D.F., J.A. MacDonald, and K. Sosin, "Microporous Carbons As Adsorbents for Methane Storage," presented at *ACS National Meeting*, SanDiego, CA, March 1994.

Remick, R.J., R.H. Elkins, E.H. Camara, and T. Bulicz, *Advanced On-Board Storage Concepts for Natural Gas-Fueled Automotive Vehicles*, Technical Report DOE/NASA/0327-1, June 1984.

Remick, R.J. and A.J. Tiller, "Advanced Methods for Low-Pressure Storage of CNG," in *Proceedings of the Nonpetroleum Vehicles Fuels Symposium*, pp. 105–119, Chicago, IL, 1985.

Remick, R.J. and A.J. Tiller, "Heat Generation in Natural Gas Adsorption Systems," presented at *Gaseous Fuels for Transportation International Conference*, Vancouver, Canada, Aug. 1986.

Sejnoha, M., R. Chahine, W. Yaïci, and T.K. Bose, "Adsorption Storage of Natural Gas on Activated Carbon," presented at *AIChE Annual Meeting*, San Francisco, USA, Nov. 1994.

Talu, O., "An Overview of Adsorptive Storage of Natural Gas," presented at *4th International Conference on Fundamentals of Adsorption*, Kyoto, Japan, May 1992.

Talu, O., *Use of Additives to Increase Adsorptive Storage Capacity*, Department of Chemical Engineering, Cleveland State University, Cleveland, Ohio, 1993.

Villadsen, J.V. and W.E. Stewart, "Solution of Boundary-Value Problems by Orthogonal Collocation," *Chem. Eng. Sci.*, **22**, 1483–1501 (1967).

Yang, R.T., *Gas Separation by Adsorption Processes*, Butterworths Publishers, Boston, MA, USA, 1987.